

# Computational Approach to Drug Design for Oxazolidinones as Antibacterial Agents

Yun Li<sup>1,2</sup>, Dong-Qing Wei<sup>1,4,\*</sup>, Wei-Na Gao<sup>2</sup>, Hui Gao<sup>2</sup>, Bing-Ni Liu<sup>3</sup>, Chang-Jiang Huang<sup>3</sup>, Wei-Ren Xu<sup>3</sup>, Deng-Ke Liu<sup>3</sup>, Hai-Feng Chen<sup>1</sup> and Kuo-Chen Chou<sup>4,\*</sup>

<sup>1</sup>College of Life Sciences and Biotechnology, Shanghai Jiaotong University, 800 Donglin Road, Minhang District, Shanghai, 200030, China; <sup>2</sup>Tianjin Institute of Bioinformatics and Drug Discovery, Tianjin Normal University, Tianjin 300074, China; <sup>3</sup>Tianjin Institute of Pharmaceutical Research, Tianjin 300193, China; <sup>4</sup>Gordon Life Science Institute, 13784 Torrey Del Mar Drive, San Diego, California 92130, USA

**Abstract:** A three dimensional Quantitative Structure Activity Relationship (3D-QSAR) model for a series of (S)-3-Aryl-5-substituted oxazolidinones was developed to gain insights into the design for potential new antibacterial agents. It was found that the Comparative Molecular Field Analysis (CoMFA) method yielded good results while the Comparative Molecular Similarity Indices Analysis (CoMSIA) was less satisfactory. The CoMFA method yielded a cross-validated correlation coefficient  $q^2 = 0.681$ , non-cross-validated  $R^2 = 0.991$ , SE (Standard Error) = 0.054, and the value of statistical significance measure  $F = 266.98$ . The relative steric and electrostatic contributions are 0.542 and 0.458, respectively. These results indicate that the model possesses a high predictivity. Guided by this model, three new compounds were synthesized. All these compounds exhibit inhibitory activity; two of them were shown having high activity (MIC = 1.0 $\mu$ g/ml). The activity observed by experiments was in good agreement with the theoretical one. It is anticipated that the present model would be of value in facilitating design of new potent antibacterial agents.

**Key Words:** 3D-QSAR, antibacterial agents, synthesis of oxazolidinones compounds.

## INTRODUCTION

Oxazolidinones have become a novel class of antibacterial agents succeeding sulfanilamides and quinolones. Linezolid, the first oxazolidinone marketed for clinical use, is remarkably effective on treating infections caused by the Gram-positive bacteria, resistant Gram-positive pathogens and certain anaerobic bacteria. However, several isolates resistant to linezolid emerged in no more than one year [1,2], so it is very urgent to develop new antibacterial agents oxazolidinones. It has been repeatedly indicated that using various computational approaches can provide valuable information for drug development (see, e.g., [3-15]), speeding up its process and reducing cost (see, e.g., [9,16-20]). Recently, some novel computational approaches, such as the cellular automaton modeling and network dynamic model, were used to study the hepatitis B viral infection [12], replication ratio by HBV virus gene missense mutation [21], analysis of SARS-CoV [22], and p53 stress response under ion radiation [23]. In this study, the 3D-QSAR method was used to design oxazolidinone analogues aiming at reducing costs, cutting down the R&D circle, and putting resources to rational use. In this paper, both CoMFA (Comparative Molecular Field Analysis), and CoMSIA (Comparative Molecular Similarity Indices Analysis) were employed to establish a 3D-QSAR model; based on the best model, several compounds were designed and three of them were synthesized. All these syn-

thesized compounds have exhibited inhibitory activity. Two of them have shown high activity (MIC = 1.0 $\mu$ g/ml). These findings can help us better understand the relationship between substituents and antibacterial activity, so as to improve the quantitative prediction of their inhibitory activities.

## COMPUTATIONAL METHODS

**Data Set.** The structures and the Minimum Inhibitory Concentration (MIC) against the staphylococcal bacteria (*S.aureus* Smith) (in  $\mu$ g/ml) were extracted from the literature [24,25]. Listed in Table 1 are the structures and MIC data for the training set.

### Molecular Modeling

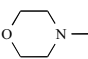
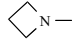
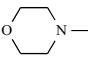
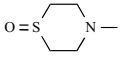
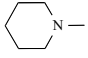
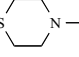
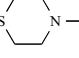
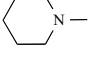
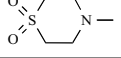
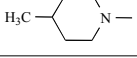
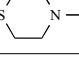
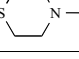
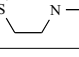
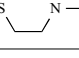
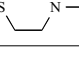
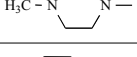
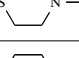
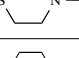
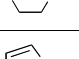
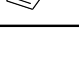
The SYBYL [26] program package was used to conduct all the modeling in this study. Conformations of compounds in the training set and test set were generated using systematic search model in SYBYL according to the four single bonds a, b, c, d with an angle increment of 15 degrees (Fig. 1). Energy minimization was performed using Tripos force field [27] with a distance-dependent dielectric and the Powell-Beale version of the conjugate gradient algorithm with a convergence criterion of 0.01 kcal/(mol Å). Partial atomic charges were calculated using the Gasteiger-Hückel method. The detailed geometry data are given in Table 2.

### Alignment Based on Pharmaphocore

Cross-validated  $q^2$  usually serves as the quantitative measurement of the prediction of CoMFA and CoMSIA. Cho *et al.* [28] reported that  $q^2$  value was sensitive to the orientation of aligned molecules and might vary with the orientation by as much as 0.5  $q^2$  units. It is therefore very

\*Address correspondence to these authors at the College of Life Sciences and Biotechnology, Shanghai Jiaotong University, 800 Donglin Road, Minhang District, Shanghai, 200030, China; E-mail: lifescience@san.rr.com  
Gordon Life Science Institute, 13784 Torrey Del Mar Drive, San Diego, California 92130, USA; E-mail: kchou@san.rr.com

Table 1. The Structural and Bioactivity of Compounds

No.	R <sub>1</sub>	R <sub>2</sub>	MIC	pMIC <sub>act</sub> <sup>a</sup>
M1	$\text{—NH—C—CH}_3$    O		6.25	1.73
M2	$\text{—NH—C—NH}_2$    S		0.78	2.62
M4	$\text{—NH—C—NH}_2$    S		1.56	2.66
M5	$\text{—NH—C—SCH}_3$    S		1.56	2.43
M6	$\text{—NH—C—SCH}_3$    S		6.25	1.79
M8	$\text{—NH—C—OCH}_2\text{CH}_3$    S		3.13	2.11
M9	$\text{—NH—C—OCH}_2\text{CH}_2\text{CH}_3$    S		50.00	0.92
M10	$\text{—NH—C—OCH}_3$    S		3.13	2.07
M11	$\text{—NH—C—OCH}_3$    S		0.78	2.73
M12	$\text{—NH—C—OCH}_3$    S		3.13	2.06
M13	$\text{—NH—C—NHNH}_2$    S		6.25	1.79
M14	$\text{—NH—C—CH}_3$    O		3.13	2.05
M15	$\text{—NH—C—NH}_2$    O		1.56	2.68
M16	$\text{—NH—C—H}$    O		6.25	1.73
M17	$\text{—NH—C—CH}_2\text{CH}_3$    O		6.25	1.77
M18	$\text{—NH—C—OCH}_3$    S		1.56	2.39
M19	$\text{—NH—C—NH}_2$    O		3.13	2.05
M20	$\text{—NH—C—NHCH}_2\text{CH}_3$    O		12.5	1.50
M21	$\text{—NH—C—CH}_3$    S		1.56	2.37
M22	$\text{—NH—C—OCH}_3$    S		0.78	2.65

a: pMIC =  $-\log(\text{MIC}/M_w)$ .

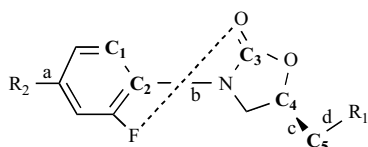


**Fig. (1).** Structures of oxazolidinones, where the dashed line refers to the O-F distance, and single bonds a, b, c, d refer to 4 rotatable bonds.

important to select suitable alignment rules for constructing 3D-QSAR model. In such cases, the 3D alignment (or superposition) of putative ligands [29,30] can be used to deduce the structural requirements for biological activity. Another strategy is the pharmacophore elucidation in which several ligands are aligned and a small collection of essential molecular features required for the biological activity is derived from the alignment. In fact, the 3D-QSAR model [31] such as CoMFA uses a 3D molecular alignment as the input. Actually, it is generally assumed for the methodologies based upon the 3D alignment for finding biologically active ligands that, if two ligands have similar biological activity and bind in a similar mode, then their bound-conformations are supposed to have a good alignment and inferences can be made

about the nature of the receptor. The alignment conducted in the current study was a stochastic search procedure that simultaneously searched the conformation space of a collection of molecules and the space of alignments of those molecules. The scoring of alignments is based upon a Gaussian density representation of pharmacophore features tuned to reproduce some certain X-ray crystallographic alignment, which includes hydrogen bond donors, hydrogen bond acceptors, cations, anions, hydrophobic area and aromatic centers. The minimization of the score function and average strain was performed to search for the best alignment of the molecules concerned. In Table 2, we found that the distance between oxygen and fluorine atom is restricted to a narrow range, i.e., 6.46 to 6.71 Å, the dihedral angle between benzene and oxazolidinone ring is  $-9.4^{\circ}$  to  $3.1^{\circ}$ , and angle  $\angle$ O-C<sub>4</sub>-C<sub>5</sub> is  $108.1^{\circ}$  to  $110.5^{\circ}$ . It is quite obvious that the structures investigated have a common pharmacophore, and hence can be aligned according to this common pharmacophore. The result thus obtained is shown in (Fig. 2).

### CoMFA Models

The CoMFA study was carried out by running the SYBYL/CoMFA module. The steric and electrostatic field en-

**Table 2.** Geometry Data of the Lowest-Energy Conformations

No.	Distance(O-F)	Dihedral C <sub>1</sub> -C <sub>2</sub> -N-C <sub>3</sub>	Angle O-C <sub>4</sub> -C <sub>5</sub>
1	6.71	-2.80	109.30
2	6.71	-0.20	110.50
4	6.70	-3.90	108.10
5	6.71	-0.40	110.50
6	6.70	-0.30	110.50
8	6.71	-0.50	110.50
9	6.72	-1.20	110.10
10	6.71	-1.00	109.20
11	6.71	1.40	110.40
12	6.68	-9.40	109.80
13	6.70	-3.30	109.70
14	6.70	1.20	110.40
15	6.70	-3.00	109.60
16	6.70	1.10	110.40
17	6.71	-2.30	109.60
18	6.71	-4.90	110.40
19	6.72	-0.30	110.10
20	6.71	-4.90	110.30
21	6.46	-6.20	109.70
22	6.69	-3.20	110.40

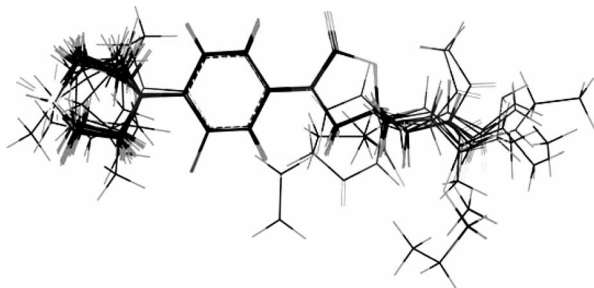


Fig. (2). The structure alignment based on a common pharmacophore.

ergies (include the type of charges) were calculated using a  $sp^3$  carbon probe atom with a charge of +1 and a distance dependent dielectric constant in all intersections of a regularly spaced (include the spacing of the grid) grid. Steric and electrostatic contributions were truncated at 30 kcal/mol. All initial partial least-squares (PLS) [32] analyses were performed using the "leave-one-out" cross-validation method. A minimum (column filter) value of 2.00 kcal/mol was set to improve the signal-to-noise ratio by omitting those lattice points whose energy variation was below this threshold. The final model (non-cross-validated conventional analysis) was developed from the model with the highest cross-validated  $r^2$ , and the optimum number of components was set to equal that yielding the highest  $q_{cv}^2$ . The final model (non-cross-validated conventional analysis) was developed from the model with the highest cross-validated  $r^2$ , and the optimum number of components was set to equal that yielding the highest  $rcv$ . The LOO cross validation should be counter-checked by a LMO one to avoid overfitting problems also considering that the diversity in the training set is not much.

### CoMSIA Models

CoMSIA similarity indices were derived with the method proposed by Klebe *et al.* [33,34] with the same lattice box

used for the CoMFA calculations. Five physicochemical properties related to steric, electrostatic, hydrophobic, hydrogen bond donor, and hydrogen bond acceptor fields were evaluated on the probe atom. Gaussian-type distance dependence was employed to describe the relative attenuation of the field's position of each atom in lattice. The use of Gaussian-type distance dependence in CoMSIA would lead to much smoother sampling of the fields around the molecules than CoMFA. The default value of 0.3 was used as the attenuation factor.

## RESULTS AND DISCUSSION

### 3D-QSAR Models

Two methods, CoMFA and CoMSIA, were used to construct the 3D-QSAR models for oxazolidinone analogues. The parameters of the two models with different grids are given in Table 3.

### Analysis of the Influence of Grids on CoMFA and CoMSIA Models

Illustrated in (Fig. 3) are the relations between cross-validated  $q^2$ , non cross-validated  $r^2$  values and the grid spaces. It can be remarked that the  $q^2$  and  $r^2$  for CoMFA models reach maximum values when grid space is 2.0 Å, suggesting that grid space could improve the models for CoMFA ( $q^2$  from 0.594 to 0.681,  $r^2$  from 0.979 to 0.991). For CoMSIA, the best model is corresponding to the grid space 1.0 Å; however, there is no significant difference between the models at 1.0 Å and 2.0 Å. Therefore the model generated with grid space 2.0 Å, which has highest non cross-validated  $r^2$  value and low SEE for training set, was chosen as the best CoMFA model.

### Analysis of CoMFA Models

The PLS statistics of CoMFA descriptor are summarized in Table 3. The steric and electrostatic field contributions are 0.548 and 0.452, respectively. Shown in (Figs. 4-5) are the

Table 3. PLS Statistics of CoMFA and CoMSIA 3D-QSAR Model

	CoMFA					CoMSIA				
	1.0 Å	1.5 Å	2.0 Å	2.5 Å	3.0 Å	1.0 Å	1.5 Å	2.0 Å	2.5 Å	3.0 Å
Grids	1.0 Å	1.5 Å	2.0 Å	2.5 Å	3.0 Å	1.0 Å	1.5 Å	2.0 Å	2.5 Å	3.0 Å
$q^2$	0.630	0.594	0.681	0.672	0.611	0.402	0.334	0.470	0.473	0.364
$r^2$	0.980	0.979	0.991	0.987	0.986	0.872	0.872	0.871	0.869	0.858
SEE	0.079	0.081	0.054	0.065	0.069	0.188	0.188	0.189	0.190	0.192
F	148.910	139.980	266.980	182.950	159.950	38.599	38.705	38.101	37.735	54.402
Components	5	6	6	5	6	3	3	3	3	2
Steric	0.567	0.561	0.548	0.563	0.487	0.059	0.059	0.058	0.055	0.056
Electrostatic	0.433	0.439	0.452	0.437	0.513	0.369	0.366	0.372	0.363	0.343
Hydrophobic	-	-	-	-	-	0.170	0.169	0.166	0.139	0.213
Donor	-	-	-	-	-	0.307	0.310	0.309	0.355	0.280
Acceptor	-	-	-	-	-	0.095	0.095	0.095	0.089	0.109

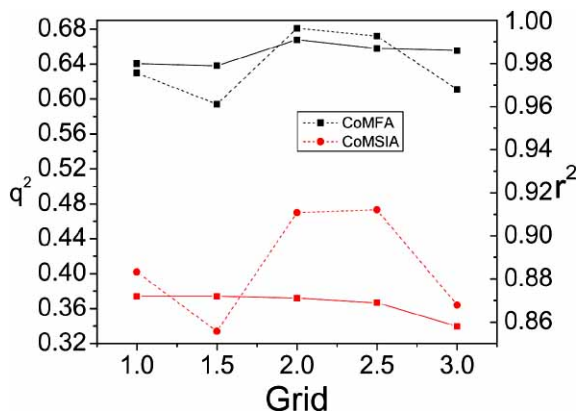


**Fig. (3).** The relations between  $q^2$  (dash curves),  $r^2$  (dash curves) and grid space used in 3D-QSAR models.

contour plots of CoMFA model. The meanings of the different colour areas are given in the legend. Red-coloured and yellow-coloured regions near position 4 of oxazolidinone ring suggest that small volume and electronegative groups are favourable to activity. The activities for the following three compounds are in the order M7> M8> M9. The bulk volumes of their corresponding substituents have the reverse order  $-\text{CH}_3$  ( $151.6\text{\AA}^3$ ) <  $-\text{CH}_2\text{CH}_3$  ( $211.1\text{\AA}^3$ ) <  $-\text{CH}_2\text{CH}_2\text{CH}_3$  ( $267.6\text{\AA}^3$ ). This is in agreement with the conclusion derived from CoMFA model. It also could explain that molecule M14 has higher activity than that of structure M17. The electronegativity of substituent ( $-\text{NH}_2$ ) is larger than that of ( $-\text{CH}_3$ ), suggesting that  $\text{NH}_2$  has stronger capacity of acceptor electron than  $\text{CH}_3$ . This could explain that M2 with substituent  $\text{NH}_2$  is more favourable to the activity than M1 with  $\text{CH}_3$ . It also could explain that the activity has the order: M10( $-\text{OCH}_3$ )>M6( $-\text{SCH}_3$ ), M15( $-\text{NH}_2$ )>M16( $-\text{H}$ ), M3( $-\text{NH}_2$ )>MM10( $-\text{OCH}_3$ ). For substituents R1, red-coloured and green-coloured regions suggest that the bulk and electronegative groups are favourable to the activity. It could explain that the activity is with the order: M7>M10, M10>M12 and M11>M18, suggesting that CoMFA model could predict and explain the training set.

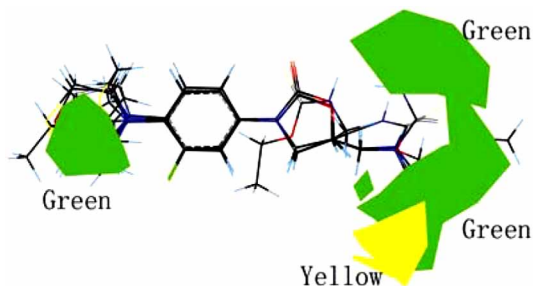


**Fig. (4).** CoMFA steric contour plots where green contours indicate regions where bulky groups increase the activity, whereas yellow contours indicate regions where bulky groups decrease the activity. (For interpretation of the references to color in this figure legend, the reader is referred to the web version of this paper).

### Design and Synthesis of New Compounds

Guided by the above CoMFA model and known pharmacophores, the novel structural modification was focused on

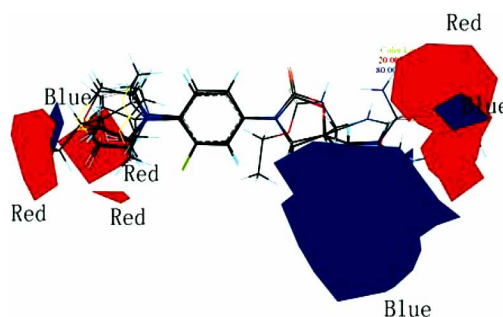


**Fig. (5).** CoMFA electrostatic contour plots where blue contours indicate regions where electropositive groups increase activity, whereas red contours indicate regions where electronegative groups may increase activity. (For interpretation of the references to color in this figure legend, the reader is referred to the web version of this paper).

the 4-substituents. Accordingly, small volume and electronegative groups are introduced into this position. Three new compounds were designed and synthesized (gathered in Table 4). The cell level bioactivity was assessed with respect to bacteria *S.aureus* Smith (CMCC26003) and tested by the Chinese National Institute for Control of Pharmaceutical and Biological Products. The experimental results are compared with theoretical prediction. And good accord has been indeed achieved as shown in Table 4 and (Fig. 6). Actually, all the designed compounds exhibited inhibitory activities with MIC values lower than  $2.00\ \mu\text{g/ml}$ . The most promising compounds are N1 and N2 with MIC values of  $1.00\ \mu\text{g/ml}$ . These two compounds were both more potent than most compounds in the same assay.

The correlation between predicted and experimental activities for newly synthesized compounds is shown in (Fig. 6). The correlation coefficient  $r$  between EA and PA is 0.927, with standard error (SE) equal to 0.16. It should be pointed out that we have only 3 newly synthesized compounds. In fact, a number of structures has been designed. But the synthesis is difficult and very cost. In this case, we have to choose the new molecules with the best predicted values for synthesis. Furthermore, our goal is not only to study theoretically the QSAR, we hope also to obtain some molecules which have the potential to be developed as drugs. This diminution in number leads to the decrease of performance. Anyhow, the tendency is good, and the prediction is relatively respected. For example, the compounds M1 and M2 are active according to the predicted values using our model. The biological assay shows that these three compounds possess good activities. Current bioassay data verified the reliability of the 3D-QSAR model described above.

The correlation between predicted and experimental activities for newly synthesized compounds is shown in Fig. (6). The correlation coefficient  $r$  between EA and PA is 0.62, with standard error (SE) equal to 0.33. We observed a decrease for  $r^2$  with respect to the constructed model using the training set. It should be pointed out that so far we have only 3 newly synthesized compounds. In fact, a number of structures have been virtually generated and designed. But the synthesis was difficult and costly. Therefore, we had to limit

Table 4. The Substituent, Predicted and Actual Activity of New Compounds

No.	R1	R2	pMIC <sub>cal</sub>	pMIC <sub>act</sub>	MIC (µg/ml)
N1			2.94	2.57	1.00
N2			2.22	2.60	1.00
N3			2.01	2.37	2.00

our choice to a few from the generated molecules that had the best predicted values for synthesis. Furthermore, our goal is not only to study the QSAR theoretically, but also to obtain some real molecules with the potential to be developed as drugs. The biological assay shows that these three compounds possess good activities, indicating that the reliability of the 3D-QSAR model described above has been verified by the current bioassay data.

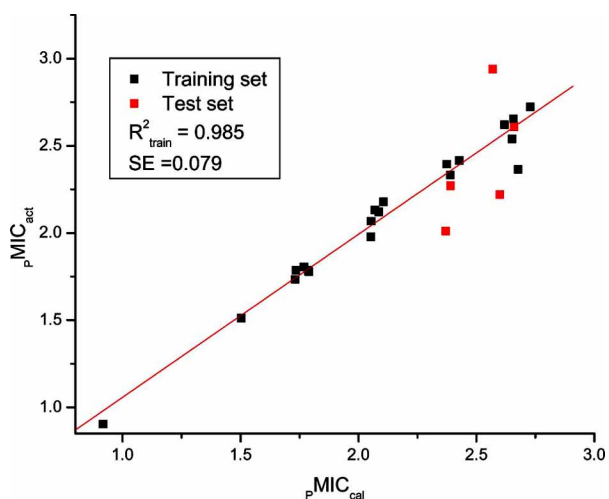


Fig. (6). The correlation between experimental and predicted activity.

## CONCLUSION

The 3D-QSAR model was developed for a class of (S)-3-Aryl-5-substituted oxazolidinones making use of CoMFA and CoMSIA. Good statistical correlation has been obtained with CoMFA, but CoMSIA did not perform well. This has to do with the fact that the main frame of these molecules is quite rigid while CoMSIA works better for flexible molecules. Our model seems, to some extent, depending on the grid used. The best result is achieved for grid = 2Å. When the grid is too fine, not only the calculations are slow, some noise in the PLS computations also gets involved making the result less accurate.

The steric and electrostatic plots provide important clues for how to design compounds potentially active. Guided by

the CoMFA model, three molecules have been designed and synthesized successfully. Their bioactivity is quite promising compared with most of the existing compounds in the training set, indicating that the results predicted by the current model agree well with the experimental observations.

## ACKNOWLEDGEMENTS

This work was supported by grants from Chinese National Science Foundation under the contract No. 10376024 and 20373048 and the Tianjin Commission of Education under the contract No. 20030001, the Tianjin Commission of Sciences and Technology under the contract No. 033801911 and special fund for intensive computation under the contract No. 043185111-4, also Virtual Laboratory for Computational Chemistry of CNIC and Supercomputing Center of CNIC, Chinese Academy of Sciences.

## REFERENCES

- [1] Gonzales, R. D.; Schreckenberger, P. C.; Graham, M. B.; Kelkar, S.; DenBesten, K.; Quinn, J. P. *Lancet*, **2001**, *357*, 1179.
- [2] Jones, R. N.; Della-Latta, P.; Lee, L. V.; Biedenbach, D. J. *Diagn. Microbiol. Infect. Dis.*, **2002**, *42*, 137-139.
- [3] Chou, K. C. *Biochem. Biophys. Res. Comm.*, **2004**, *316*, 636-642.
- [4] Du, Q. S.; Wang, S. Q.; Jiang, Z. Q.; Gao, W. N.; Li, Y. D.; Wei, D. Q.; Chou, K. C. *Med. Chem.*, **2005**, *1*, 209-213.
- [5] Chou, K. C. *J. Proteome Res.*, **2004**, *3*, 1284-1288.
- [6] Wei, D. Q.; Zhang, R.; Du, Q. S.; Gao, W. N.; Li, Y.; Gao, H.; Wang, S. Q.; Zhang, X.; Li, A. X.; Sirois, S.; Chou, K. C. *Amino Acids*, **2006**, *31*, 73-80.
- [7] Chou, K. C. *Anal. Biochem.*, **1996**, *233*, 1-14.
- [8] Wang, S. Q.; Du, Q. S.; Zhao, K.; Li, A. X.; Wei, D. Q.; Chou, K. C. *Amino Acids*, **2006**, DOI 10.1007/s00726-00006-00403-00721.
- [9] Chou, K. C.; Wei, D. Q.; Zhong, W. Z. *Biochem. Biophys. Res. Comm.*, **2003**, *308*, 148-151.
- [10] Zhang, R.; Wei, D. Q.; Du, Q. S.; Chou, K. C. *Med. Chem.*, **2006**, *2*, 309-314.
- [11] Chou, K. C.; Watenpugh, K. D.; Heinrikson, R. L. *Biochem. Biophys. Res. Comm.*, **1999**, *259*, 420-428.
- [12] Xiao, X.; Shao, S. H.; Chou, K. C. *Biochem. Biophys. Res. Comm.*, **2006**, *342*, 605-610.
- [13] Du, Q. S.; Sun, H.; Chou, K. C. *Med. Chem.*, **2007**, *3*, 1-6.
- [14] Chou, K. C.; Tomasselli, A. G.; Heinrikson, R. L. *FEBS Lett.*, **2000**, *470*, 249-256.
- [15] Wei, H.; Zhang, R.; Wang, C.; Zheng, H.; Chou, K. C.; Wei, D. Q. *J. Theoretical Biol.*, **2007**, *244*, 692-702.
- [16] Chou, K. C. *Curr. Med. Chem.*, **2004**, *11*, 2105-2134.
- [17] Sirois, S.; Wei, D. Q.; Du, Q. S.; Chou, K. C. *J. Chem. Inf. Comput. Sci.*, **2004**, *44*, 1111-1122.
- [18] Sirois, S.; Hatzakis, G. E.; Wei, D. Q.; Du, Q. S.; Chou, K. C. *Comput. Biol. Chem.*, **2005**, *29*, 55-67.

- [19] Chou, K. C.; Wei, D. Q.; Du, Q. S.; Sirois, S.; Zhong, W. Z. *Curr. Med. Chem.*, **2006**, *13*, 3263-3270.
- [20] Sirois, S.; Tsoukas, C. M.; Chou, K. C.; Wei, D. Q.; Boucher, C.; Hatzakis, G. E. *Med. Chem.*, **2005**, *1*, 173-184.
- [21] Xiao, X.; Shao, S.; Ding, Y.; Huang, Z.; Chen, X.; Chou, K. C. *J. Theoretical Biol.*, **2005**, *235*, 555-565.
- [22] Wang, M.; Yao, J. S.; Huang, Z. D.; Xu, Z. J.; Liu, G. P.; Zhao, H. Y.; Wang, X. Y.; Yang, J.; Zhu, Y. S.; Chou, K. C. *Med. Chem.*, **2005**, *1*, 39-47.
- [23] Qi, J. P.; Shao, S. H.; Li, D. D.; Zhou, G. P. *Amino Acids*, **2006**, DOI 10.1007/s00726-00006-00454-00723.
- [24] Tokuyama, R.; Takahashi, Y.; Tomita, Y.; Suzuki, T.; Yoshida, T.; Iwasaki, N.; Kado, N.; Okezaki, E.; Nagata, O. *Chem. Pharm. Bull. (Tokyo)*, **2001**, *49*, 347-352.
- [25] Tokuyama, R.; Takahashi, Y.; Tomita, Y.; Tsubouchi, M.; Yoshida, T.; Iwasaki, N.; Kado, N.; Okezaki, E.; Nagata, O. *Chem. Pharm. Bull. (Tokyo)*, **2001**, *49*, 353-360.
- [26] SYBYL *Tripos Associates Inc, Version 7.0, St. Louis (MO)*.
- [27] Cramer, R. D., 3rd; Patterson, D. E.; Bunce, J. D. *Prog. Clin. Biol. Res.*, **1989**, *291*, 161-165.
- [28] Cho, S. J.; Tropsha, A. *J. Med. Chem.*, **1995**, *38*, 1060-1066.
- [29] Martin, Y. C.; Bures, M. G.; Danaher, E. A.; DeLazzer, J.; Lico, I.; Pavlik, P. A. *J. Comput. Aided. Mol. Des.*, **1993**, *7*, 83-102.
- [30] Miller, M. D.; Sheridan, R. P.; Kearsley, S. K. *J. Med. Chem.*, **1999**, *42*, 1505-1514.
- [31] Pae, A. N.; Kim, S. Y.; Kim, H. Y.; Joo, H. J.; Cho, Y. S.; Choi, K. I.; Choi, J. H.; Koh, H. Y. *Bioorg. Med. Chem. Lett.*, **1999**, *9*, 2685-2690.
- [32] Stahle, L.; Wold, S. In *Progress in Medicinal Chemistry*; Ellis, G. P., West, G. B., Eds.; Elsevier, **1988**.
- [33] Klebe, G.; Abraham, U. *J. Comput. Aided Mol. Des.*, **1999**, *13*, 1-10.
- [34] Bohm, M.; St rzebecher, J.; Klebe, G. *J. Med. Chem.*, **1999**, *42*, 458-477.